3.2.3

Thermal hydraulic design of a double-walled mercury target vessel by simulations and water experiments

K Haga, T Naoe, T Wakui, H Kogawa, H Kinoshita and M Futakawa

J-PARC Center, JAEA, Tokai, Ibaraki 319-1195, Japan.

E-mail: haga.katsuhiro@jaea.go.jp

Abstract. To mitigate the cavitation damage of the mercury target vessel operating at the spallation neutron source of J-PARC, a double-walled structure for the target vessel was investigated and designed by numerical simulation. It was found that rapid mercury flow in the narrow channel at the beam window and sufficient cooling performance of the target wall were attained. Moreover, the rapid mercury flow might be maintained even in the case of an inner-wall fracture. These results were found to be consistent with the water experiments in the case of small damage of the inner wall.

1. Introduction

In the mercury target of the pulsed spallation neutron source of J-PARC, injections of high-power (1 MW) pulsed proton beam induce pressure waves in the mercury and cause cavitation damage to the target vessel wall, which is a crucial issue for stable system operation [1]. To mitigate cavitation damage, a microbubble injection technique, which reduces the intensity of the pressure waves, has been developed. A microbubble generator, also called a bubbler, was developed to generate microbubbles with a diameter less than 100 μm in the mercury; it has been used in the mercury target system of J-PARC since October 2012. Using a Laser-Doppler vibrometer, it was found that the displacement velocity of the target vessel was reduced to 1/3 on average at the proton beam power of less than 300 kW, which showed the efficacy of the microbubble injection.

For the further development of the high-power target, we focused on the mercury flow effect to mitigate the cavitation damage. So far, the analytical and experimental studies [2,3,4] and the operational experiences of Spallation Neutron Source (SNS) [5] suggest that rapid mercury flow can mitigate the cavitation damage. To include these effects in the target design of J-PARC, we developed a double-walled structure and applied it to the beam window, which is the forefront tip of the target vessel. The mercury flow channel, with a narrow gap of 2 mm, was made by adding an inner wall just inside the beam window.

In this report, thermal hydraulic design of the double-walled target by simulations and the results of the water experiments using the mock-up model are presented, including the case of failure of the inner wall.

2. Double Wall Concept to Extend the Lifetime of the Beam Window

Figure 1 shows a schematic of the structure of the double-walled target vessel (top view). Based on experimental data [6], though it is under the stagnant condition, the effect of pitting damage mitigation becomes better as the channel gap is smaller, because the channel walls can disturb the inflation of

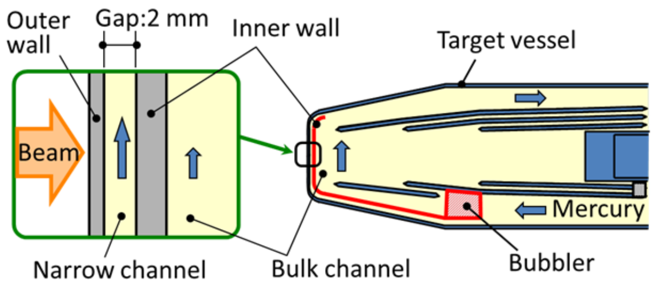

Figure 1. Structure of the double-walled target and the magnified view of the beam window

cavitation bubbles before they fully expand. Moreover, the effect of the fast mercury flow to deform the cavitation bubbles will reinforce the performance of the narrow channel to mitigate the pitting damage. On the other hand, the channel gap should be decided considering the manufacturing tolerance. Considering these conditions, the gap of the narrow channel was decided to be 2 mm at the beam window.

The mercury flow is separated into two channels at the bubbler, i.e., the narrow channel and the bulk channel, and they join again downstream of the beam window. Although the narrow channel is a straightforward channel with no obstacles, the bulk channel is equipped with the bubbler, which is the primary flow-resistant component in the target vessel. The maximum pressure drop at the bubbler is assumed to be 0.2 MPa considering the mercury pump performance. The mercury velocity in the narrow channel increases until the pressure drop becomes the same as that in the bulk channel, which makes the mercury velocity in the narrow channel faster than that in the bulk channel.

The merit of the double-walled structure is that the inner wall is not the mercury containment boundary, and enough cooling efficiency is expected because both sides of the inner wall are cooled by the mercury flow. This merit expands the freedom of the inner wall design for applying technologies in order to mitigate the cavitation damage on the inner surface of the inner wall. Furthermore, sufficient cooling efficiency of the inner wall enables the wall thickness to be increased, which has the advantage of enabling an increase in the erosion allowance. In the present design, the thickness of the outer wall is 3 mm and that of the inner wall is 5 mm. All these merits lead to a longer lifetime for the target vessel.

3. Target Design by Simulation

3.1. Design requirements and concerns

The design requirements for the thermal hydraulic design of the double-walled mercury target are as follows:

- A high-velocity flow field throughout the narrow channel to achieve the pitting damage mitigation effect.
  - --- In the experiences of SNS target operation, serious damages were not observed on the inner surface of the beam window cooling channel where the mercury flows at 3 m/s at maximum. Based on this fact, the design criterion for the minimum mercury velocity in the narrow channel was set at 3 m/s.
- Sufficient cooling performance which causes no serious temperature rise throughout the mercury target vessel.
  - --- The maximum temperature of the target in the past design was around 200 °C. The temperature of the target in new design should not exceed this value so much.

There are also concerns for the fabrication and the operation of the target vessel as follows:

- Influence of fabrication tolerance on the flow velocity in the narrow channel.
- Influence of inner wall failure to the mercury flow and the wall cooling.

Evaluation results of these items are shown in the following sections.

3.2 Simulation model and conditions

The commercial base thermal hydraulic code—ANSYS FLUENT—was used to analyze the time-averaged thermal hydraulics in the target model. The analytical model was a three-dimensional full model. The cell shape was tetrahedral and the total cell number was 22 million. The turbulence model was realizable k–ε model and the wall boundary condition was the law-of-the-wall.

The inlet mercury temperature was set to 50 °C. Based on experimental data, the pressure drop coefficient of the bubbler was set to 8.1, which led to a mercury velocity at the model inlet of 1.025 m/s in order to make the pressure drop at the bubbler 0.2 MPa. The volumetric heat generation was considered under the condition of the proton beam energy and power of 3 GeV and 1 MW, respectively. The proton beam profile was assumed to be Gaussian, and the maximum heat density was 430 W/cm^3 in the mercury near the beam window. The thermal condition at the outer wall boundary was set to adiabatic. The buoyancy of mercury was not considered in this analysis, because in a forced convection flow with a high Reynolds number, which is on the order of 10^5 in this case, inertial force is the dominant factor to determine the flow field and the effect of buoyancy is considered to be negligible. The turbulent Prandtl number was set to 1.5. The temperature dependency of the physical properties of mercury and stainless steel was considered.

3.3 Mercury flow field and temperature distribution

Figure 2 and Figure 3 show the simulation results of the flow field and the temperature distribution at the horizontal cross section. While the mercury velocity is ca. 1.5 m/s in the bulk channel, it is almost 4 m/s in the narrow channel at the beam window. The maximum wall temperature is 157 °C at the outer surface of the outer wall, which is not high enough to cause any problems. The maximum temperature of the inner wall, though it is somewhat thicker, is lower than that of the outer wall because it is cooled on both sides. The mercury temperature is around 60 °C in the area near the beam window and increases to 120 °C at 500 mm in the X position. Figure 4 shows the mercury flow velocity distribution in the narrow channel, which is in the vertical cross section at the center position of the beam window. Looking at the angle from −80° to 80°, we found that the flow velocity is fast (>3.5 m/s) at the center of the beam window, where rapid velocity is specially needed for the cavitation damage mitigation. The flow velocity decreases sharply at −90° and 90°. The intensity of the cavitation is assumed to be relatively weak in these regions. The flow velocity deductions seen at −30° and 30° are caused by the wake flow of the reinforcement ribs fixed in the entrance region of the

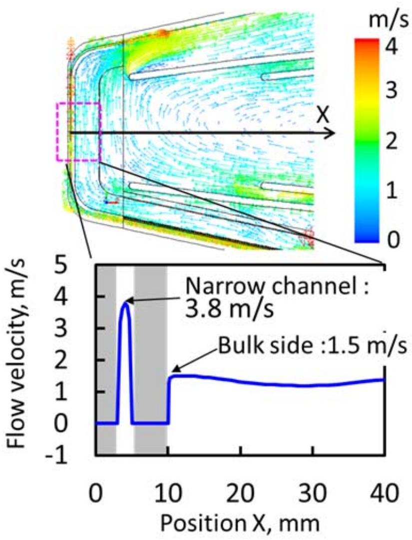

Figure 2. Mercury flow field near the beam window on the horizontal cross section

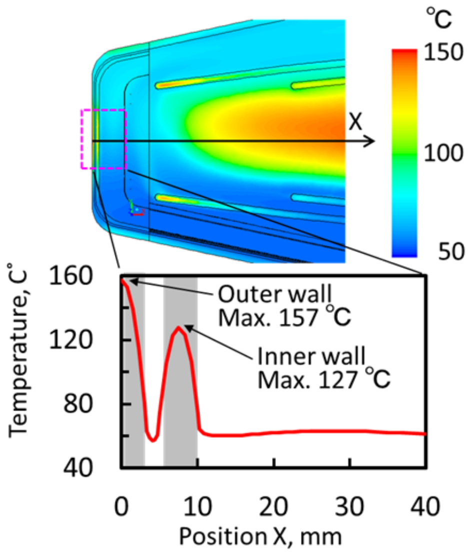

Figure 3. Temperature distribution on the horizontal cross section

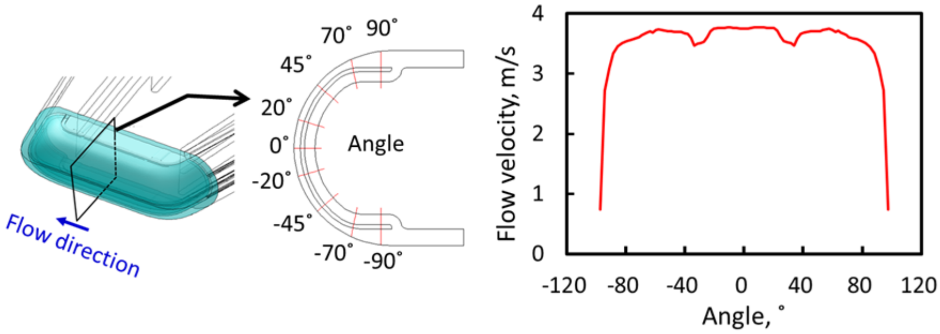

Figure 4. Mercury flow velocity distribution in the narrow channel in the vertical cross section at the center position of the beam window

narrow channel.

These results show that the design requirements of the double-walled target are fulfilled.

3.4 Influence of the fabrication tolerance of the narrow channel on the flow distribution

Because the target vessel is fabricated by welding many stainless steel parts, deformation due to the welding heat have to be considered. Because the gap of the narrow channel is small, 2 mm, the influence of the fabrication tolerance on the flow distribution should be evaluated in advance. Figure 5 shows the evaluated cases and the results. The angle in the horizontal axis of the graph has the same meaning as shown in Figure 4. In the simulation, two types of deformations were assumed, i.e., the forward and downward deformation. The models of these deformation patterns are such that the inner wall moved forward and downward respectively as shown in the upper figures in Figure 5. The channel gaps assumed in these cases are also shown in Figure 5. The flow velocity distributions in the vertical cross sections at three different positions were evaluated: the beam window center and 35 mm upstream and downstream from the center. Note that only the beam window region of the target vessel was modeled in this simulation to save the simulation cost, but the flow velocity distribution is well simulated, which can be understood by comparing Figure 4 and Figure 5 (a).

In the case of no deformation, the flow velocity distributions are fairly uniform at all cross sections

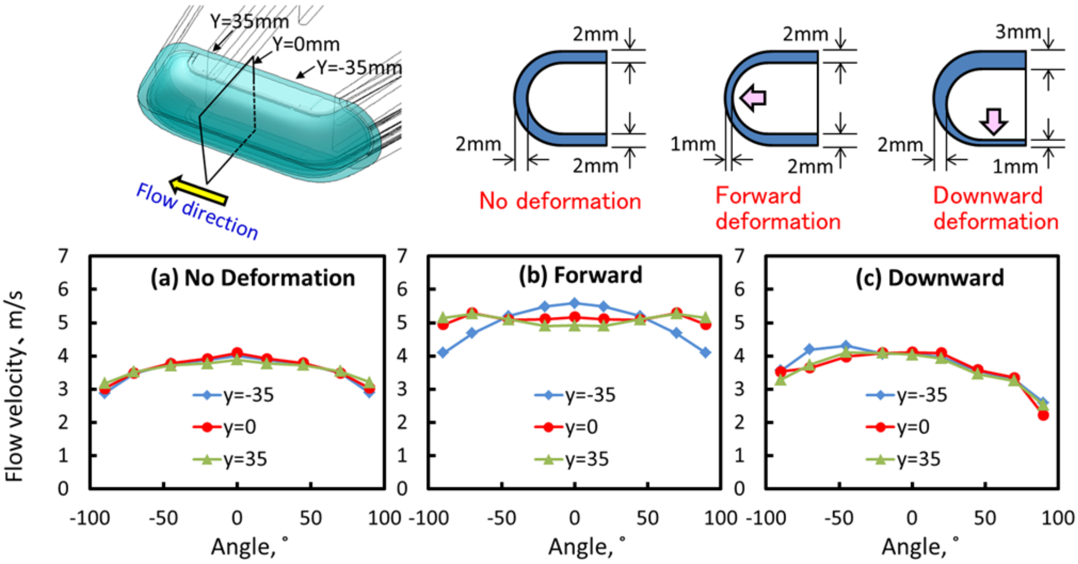

Figure 5. Deformation patterns of the inner wall and their influence on the flow distribution in the narrow channel

and are faster than 3 m/s. In the case of forward deformation, the average flow velocity increases at all cross sections because of the reduction in the cross sectional area of the flow channel. This result is advantageous for the cavitation damage mitigation. In the case of downward deformation, the flow velocity at the bottom side increased somewhat compared with the case of no deformation, but at the top side, where the channel gap increased to 3 mm, the flow velocity decreased to 2 m/s at all cross sections. This result indicates that special attention should be paid to the deformation that makes the channel gap broader, because it leads to reduction in the flow velocity.

3.5 Influence of inner wall fracture on the flow field

Because the efficacy of micro-bubbles to mitigate the cavitation damage has not yet been confirmed quantitatively in the actual mercury target, the possibility of inner wall fracture has to be considered. The inner wall fracture was modeled by a circular hole in the inner wall at the center of the beam window, and the influence of the hole on the flow fields in the narrow and bulk channels was evaluated. The hole diameter was assumed to be 10 mm and 30 mm. Figure 6 shows the simulation results. Surprisingly, the mercury flow velocity in the narrow channel at the center of the beam window does not decrease much, and the velocity is kept well over 3 m/s even in the case of a 30-mm hole diameter. The ratio of the amount of mercury flow outgoing to the bulk channel from the narrow channel, which is called the branch flow, is only 0.2% and 2.7% for the 10-mm and 30-mm holes, respectively.

Figure 7 shows the pressure distribution at the center axis of the hole. For the 10–mm hole, the pressure difference in the narrow and the bulk channel is very small near the region of the hole, which suppresses the branch flow. For the 30–mm hole, there is a pressure gradient descending to the bulk channel from the narrow channel, which causes the branch flow of 2.7%.

These results indicate that the effect of rapid mercury flow in the narrow channel to mitigate the cavitation damage is kept even if a damage hole penetrates the inner wall at the beam window. Of course, the shape of the damage hole and edge might influence the flow field in the narrow channel, but as a matter of fact, it was observed at SNS that the outer wall of the narrow channel was not damaged, and the inner wall had damages penetrating throughout the wall thickness. Thus, there is a possibility of double-walled target structure having a hole originally at the center of the beam window of the inner wall.

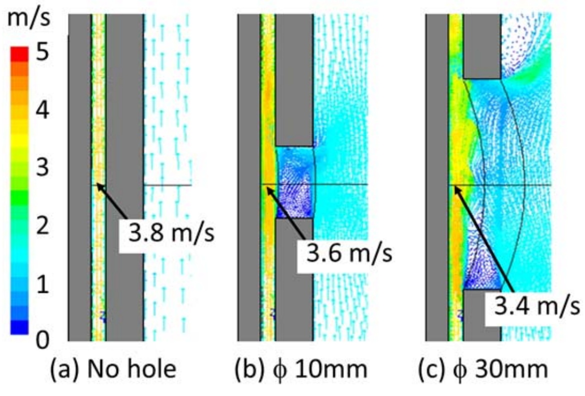

Figure 6. Mercury flow fields in the case of inner wall fracture. The fracture was modelled by a circular hole at the center of the beam window.

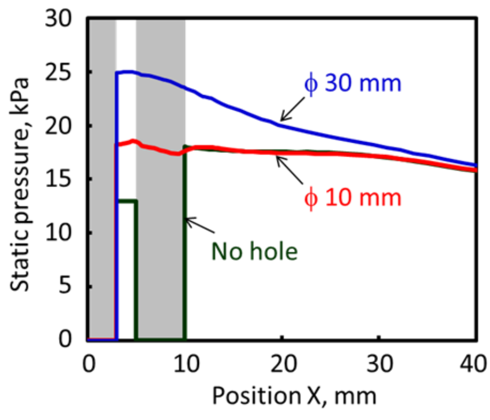

Figure 7. Pressure distribution along the center axis of the beam window (x axis is the same as Figure 1 and Figure 2).

4. Water experiments using a mock-up model

4.1. Experimental setup

In order to verify the simulation results shown above, water experiments using the mock-up model of the double walled target were carried out. The model was made of transparent acrylic resin to be used for the visualization experiment. The inner structure and the size were the same with the actual target, but the wall thickness was much thicker to ensure the structural strength against the inner pressure of around 0.2 MPa. The target model was set horizontally and the water flow velocity in the narrow channel of the double wall was measured by processing the images taken by the high speed video camera. Bubbles of ca. 0.5 mm in diameter were injected at the upstream of the narrow channel as the seeding particles to measure the water flow velocity by image processing. The high speed video camera was set at the upper side of the model to get clear image of bubbles as shown in Figure 8. The water flow velocities were measured at the areas of upstream and downstream of the beam window center to investigate the influence of the hole at the beam window simulating the inner wall fracture. The field of view was square with the dimensions of 50 mm x 50 mm.

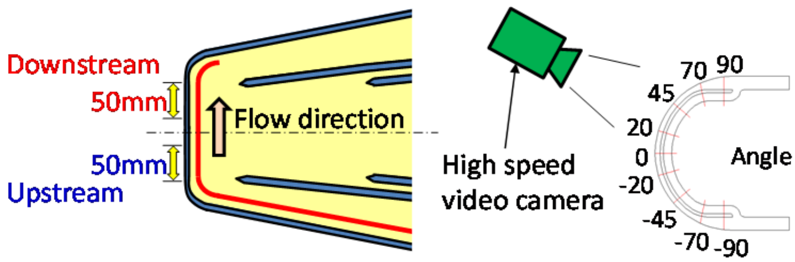

Figure 8. Focused area of video camera on the water experimental model

4.2. Experimental results

When the water velocity is very high, which is more than 10 m/s, the clear image of the bubble flow cannot be obtained even if the flame rate of the video camera is maximized. Thus, the experiments were carried out with the water flow velocity of around 6 m/s in the narrow channel, which corresponds to the water flow rate of 1050 L/min at the inlet of the target model. The water flow velocity was 1.85 m/s and the Reynolds number at the target inlet was 213000, which is 1/5 of mercury flow condition in actual target. Just the same way as the simulation, the fracture of the inner wall was modelled by a circular hole at the center of the beam window. Three cases were measured, which are no hole, 10 mm and 30 mm in diameter.

Figure 9 shows the results of the water experiments. In the case of no hole, the flow velocity is fairly

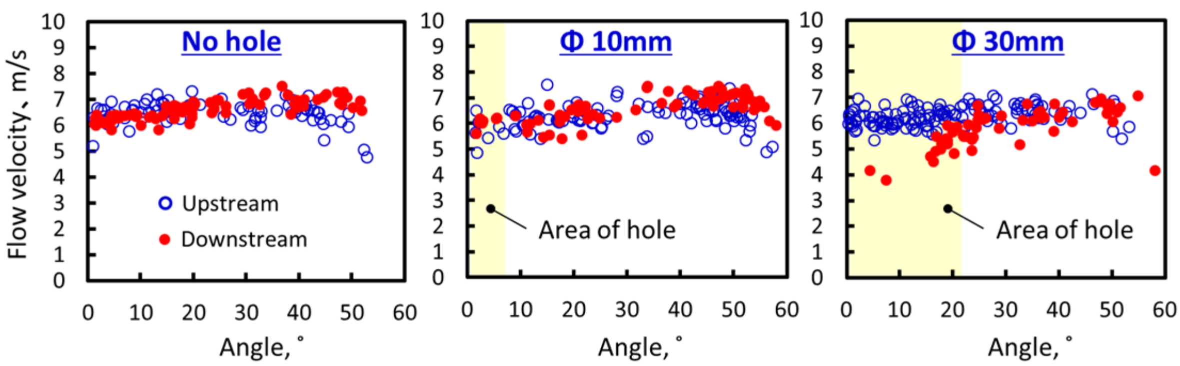

Figure 9. Results of the water experiments
(Water flow rate at model inlet : 1050 L/min)

uniform across the angle position. In the case of 10 mm, no obvious flow velocity change was detected at both the upstream and the downstream, which indicates that the inner wall fracture of 10 mm in diameter does not disturb the flow field in the narrow channel so much. These results are consistent with the simulation results shown in the former chapter. But in the case of 30 mm, the flow velocity decreased by 30 % at downstream of the modelled hole. The velocity reduction is larger than that evaluated by the simulation and the cause of the difference will be investigated by water simulation. It was found that the flow velocity in the narrow channel is not disturbed by the small damage of the inner wall, which suggests that the effect of cavitation damage mitigation can be maintained.

5. Summary

Evaluation of the thermal hydraulic design of a double-walled target vessel was performed by numerical simulations, and the items shown below were found:

1) A rapid mercury flow velocity of almost 4 m/s in the narrow channel was attained at the beam window, which might lead to the damage mitigation of the wall.
2) The effect of the double-walled structure to promote the cooling performance of the target vessel was confirmed, making it possible to increase the inner wall thickness.
3) When setting the fabrication tolerance of the narrow channel, special attention should be paid to the deformation that makes the channel gap broader, thereby leading to the reduction in the flow velocity.
4) Fast flow velocity in the narrow channel is maintained even at a fractured place open to the bulk channel, and the amount of mercury flowing out of the narrow channel to the bulk side is very small.

The water experiments were carried out to verify the simulation results with the Raynolds number of 1/5 of the actual mercury target, and the items shown below were found:

5) The flow velocity is fairly uniform across the angle position.
6) The inner wall fracture of 10 mm in diameter does not disturb the flow field in the narrow channel so much. These results are consistent with the simulation results.

6. References

[1] M. Futakawa, et.al.: Nucl. Instr. and Meth., A 562 (2006) p.676.
[2] M. Futakawa, et.al.: J. Nucl. Sci. Technol., Vol. 45 (2008) No. 10, p.1041.
[3] B. Riemer, et al.: J. Nucl. Mater., 377(2008) p.162.
[4] B. Riemer, et al.: J. Nucl. Mater., 398 (2010) p.207.
[5] D. McClintock, et al.: J. Nucl. Mater., 431(2012) p.147.
[6] T. Naoe, et.al.: Transactions of the JSME, Vol. 80 (2014) No. 810, fe0025. (in Japanese.)